Rare Metal Materials and Engineering
Volume 49, Issue 3, March 2020
Available online at www.rmme.ac.cn

Science Press

Cite this article as: Rare Metal Materials and Engineering, 2020, 49(3): 0857-0861.

ARTICLE

Effects of Different Deposition Strategies on Prior-β Grain Morphology of Wire and Arc Additive Manufactured Ti-6Al-4V Components

Wang Jian[1,2], **Lin Xin**[1,2], **Xue Aitang**[1,2], **Zhou Yinghui**[1,2], **Huang Weidong**[1,2]

[1] State Key Laboratory of Solidification Processing, Northwestern Polytechnical University, Xi'an 710072, China; [2] Key Laboratory of Metal High Performance Additive Manufacturing and Innovative Design, MIIT China, Northwestern Polytechnical University, Xi'an 710072, China

Abstract: Macrostructural characterization was performed for Ti-6Al-4V components fabricated by wire and arc additive manufacturing (WAAM) to investigate the effects of different deposition direction and interlayer dwell time on prior-*β* grain morphology. The bidirectional and unidirectional travel directions led to different growth directions of columnar prior-*β* grains. By extending the interlayer dwell time between each deposited layer to 120 s, the full equiaxed prior-*β* grains were obtained. The results indicate that the equiaxed prior-*β* grains at the bottom of the deposited wall are caused by recrystallization. The sizes of the equiaxed prior-*β* grains at the bottom are both affected by the thermal cycle and the recrystallization.

Key words: wire and arc additive manufacturing; Ti-6Al-4V; prior-*β* grain morphology; recrystallization

Titanium alloys are prevalent materials and widely used in various fields especially in the aerospace industry for their high strength-to-weight ratio, excellent corrosion and thermal resistance[1]. However, the properties such as low thermal conductivity, high chemical activity and strength, additionally, the large scale, complex shape and small quantities for the aerospace component, make it difficult and costly to fabricate them via conventional forging and casting[2]. Compared with conventional manufacturing methods, wire and arc additive manufacturing (WAAM) in additive manufacturing (AM) is a novel net shape forming technology and has been attractive to industry, possessing the characteristics of high efficiency and low cost, especially more suitable for large-scale components[3].

The high thermal gradient, complex thermal history, rapid heating and cooling lead to the elongated columnar prior-*β* grains with a strong <001> solidification texture grown epitaxially in the building direction, particularly for Ti-6Al-4V in titanium alloys[4,5]. While different from wrought components exhibiting fine equiaxed prior-*β* grains, there is significant mechanical property anisotropy in components manufactured by AM; in general, the yield and ultimate tensile strength of the component in scanning orientation are higher than those in transverse orientation, whereas the elongation shows an opposite trend[5-7]. Carroll et al.[5] pointed out that the anisotropy may be a result of discontinuous grain boundary *α* phase and the preferentially oriented prior-*β* grain boundaries. Wang et al.[8] considered that loaded transverse to the prior-*β* grain boundaries promote premature failure through the grain boundary *α* layer that results in the anisotropy. Recently, the rolling applied in-process during WAAM can significantly refine prior-*β* grains and eliminate the undesirable macrostructure to get the fine equiaxed prior-*β* grains with weakened texture. The isotropic and superior mechanical properties were obtained and better than those of the wrought material[9,10]. Besides, the microstructure of AMed component is also detrimental to fatigue life and slightly inferior to the wrought standard[1,11]. So prior-*β* grain morphology control, especially getting equiaxed

---

Received date: March 29, 2019
Foundation item: National Key Research and Development Program (2016YFB1100104)

Corresponding author: Lin Xin, Ph. D., Professor, School of Materials Science and Engineering, Northwestern Polytechnical University, Xi'an 710072, P. R. China, E-mail: xlin@nwpu.edu.cn

prior-β grains, is of great significance.

In the present work, three Ti-6Al-4V components were manufactured via WAAM with different travel directions and dwell time of each deposited layer. The effects of different deposition strategies on prior-β grain morphology were discussed and the final purpose was to improve the mechanical properties by getting the equiaxed prior-β grains.

1 Experiment

The experimental WAAM setup (Fig.1a) based on gas tungsten arc welding (GTAW) mainly consists of an EWM Tetrix521 welding machine, Tetrix 4L wire feeder and a torch mounted on a 4-axis LPM-408 CNC workbench. The deposition was carried out within an airtight chamber filled with argon (99.999% purity). In order to obtain a stable shape of the components, the following deposition parameters were used: an electrical current of 140 A, a travel speed of 250 mm/min, a wire feed speed of 1200 mm/min. Hot rolled Ti-6Al-4V substrates with 140 mm (length) × 50 mm (width) × 6 mm (thickness) were used for the deposits. Thirty layers of Ti-6Al-4V alloy were deposited for each wall with different strategies as follows: an bidirectional travel direction was applied to wall A while only unidirectional travel direction to wall B and wall C, the interlayer dwell time were 0, 24, 120 s and the dimensions of each obtained deposited wall were 100 mm×9.6 mm×22.8 mm, 100 mm×7.6 mm×28.8 mm, 100 mm×7 mm×31.2 mm, respectively.

2 Results and Discussion

2.1 Prior-β grain morphology

Fig.1a shows schematic of the setup and location of extracted specimen for macrostructure. Fig.1b~1d present the different prior-β grain morphologies of the specimens deposited with different deposition strategies. From the cross-section of walls A and B, there is an equiaxed prior-β grain zone at the bottom and then convert to the columnar prior-β grain zone at the top region. The equiaxed prior-β grains are finer near the substrate and gradually coarser along the building direction. The growth orientations of the coarse columnar prior-β grains are vertical in wall A, and tilted away from the building direction by about 9° in wall B. The significant difference for wall C is that the entire cross-section are mostly equiaxed or near equiaxed prior-β grains, and the epitaxial growth characteristic disappears.

2.2 Mechanism of the prior-β grain morphology evolution

It seems that the whole WAAM process begins to form equiaxed prior-β grains at first, and then gradually they convert to columnar prior-β grains with the increase of the height. Fig.2 shows that several layers are deposited to further study the evolution of prior-β grain morphology. Different deposition strategies result in the following various prior-β grain evolution processes: there are mostly columnar prior-β grains during the deposition of the first six layers in wall A (Fig.2a~2c) while full of equiaxed prior-β grains for wall B (Fig.2f) and wall C (Fig.2h). The columnar prior-β grains are directly epitaxially grown from the substrate (Fig.2a and 2d), indicating that there is no nucleation within the melt pool due to the insufficient undercooling, although there is the largest nucleation rate in the first layer. Therefore, the equiaxed prior-β grains are not caused by nucleation. On the other hand, the thermal gradient within the melt pool is gradually decreased during the deposition process, which promotes the columnar to equiaxed transition (CET). Nevertheless, there are merely columnar prior-β grains at the top part of the wall A and wall B. The thermal gradient within the melt pool of wall C is larger than that of wall A and wall B that is less likely to occur with CET. Therefore, there are other reasons leading to the formation of equiaxed prior-β grains. As a result, the formation of equiaxed prior-β grains is independent of nucleation or CET within the melt pool. By contrasting the prior-β grain morphology of Fig.2a and 2c, Fig.2e and 2f, Fig.2g and 2h, it can be concluded that the equiaxed prior-β grains convert to columnar prior-β grains owing to recrystallization.

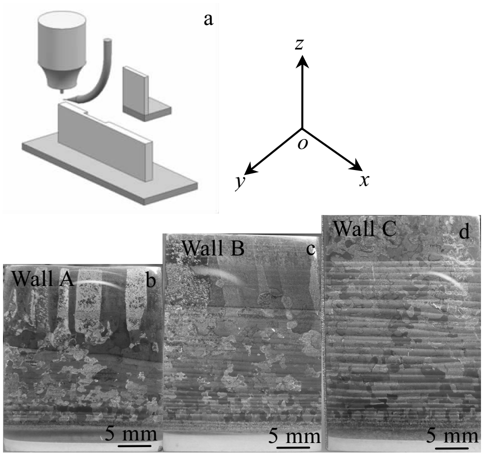

Fig.1 Schematic of the setup and location of extracted specimen for macrostructure (a) and the optical macrographs on x-z plane (b~d): (b) wall A, (c) wall B, and (d) wall C

There are many factors that promote recrystallization during WAAM process, such as large stress, high annealing temperature and heating rate. The temperature and stress are important factors affecting recrystallization. As shown in Fig.3, the high temperature leads to the low stress; therefore, they restrict each other. Both the recovery and recrystallization are thermally activated processes, whose driving force is provided with the stored energy of deformation. The effect of temperature on microstructure evolution has two main aspects: on the one hand, the increasing

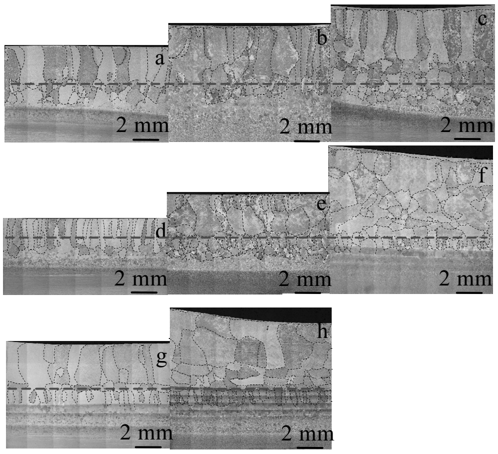

Fig.2 Optical macrographs of the different layers: (a) once, (b) twice, and (c) thrice in back and forth direction with the same deposition conditions of wall A; (d) one layer, (e) three layers, and (f) six layers with the same deposition conditions of wall B; (g) three layers, (h) six layers with the same deposition conditions of wall C

temperature intensifies the atom diffusion process, then more recovery occurs at higher temperatures and the driving force for recrystallization decreases. A significant amount of prior recovery may in turn influence the nature and the kinetics of recrystallization[12]. On the other hand, the migration ability of the prior-β grain boundary is enhanced and the incubation time of recrystallization is shortened, as well as both the recrystallization nucleation rate and the prior-β grain growth rate are increased. The local storage energy E can be approximately calculated as[13]:

$$E \approx \rho_b G b^2/2 = 3\varphi b G/2d \tag{1}$$

where G is the shear modulus; b is the Burgers vector magnitude; ρ_b is the position of the dislocation density at the grain boundaries; φ is misorientation between the deformation zone; d is the deformation zone width. When the stress and strain increase, the misorientation of φ in the vicinity of the grain boundary increases and the width of the deformation band of d decreases; therefore E increases with the increase of stress. High-density of dislocations and dislocation tangles contribute to recrystallization observed in the deposit with six layers (Fig.4a). Besides, during the depositing of the first several layers, rapid cooling of a melt pool occurring via the substrate promote the formation of supersaturated fully α' martensitic structure which also had high stored energy[14]. Therefore, a comprehensive analysis of the effect of temperature, stress, and the interaction between them on the recrystallization is needed.

As illustrated in Fig.3, the temperature is in the order of wall A > wall B > wall C at the bottom, while the stress shows the opposite trend, i.e., wall C > wall B > wall A. Only the longitudinal (travel direction) stress of the component is calculated for it is dominant throughout the wall and substrate[15,16]. Recovery, recrystallization and growth of prior-β grains occur immediately during the beginning of deposition (Fig.2f and 2h). However, no recrystallization occurs in the first six layers of wall A (Fig.2c). This is because the stress under high temperature is too weak to bring about sufficient stored energy. At this moment, only much recovery prefers to occur, the annihilation and rearrangement of dislocations are achieved by glide, climb and cross-slip, and the stored energy is consumed and becomes lower. It should be noted that recovery and recrystallization are competing processes because both of them are driven by the stored energy of the deformed state. Titanium alloys have high fault energy owing to strong recovery process, so the recrystallization is suppressed and will occur at higher temperature and need longer time. As shown in Fig.1b, the bottom of wall A recrystallizes to equiaxed prior-β grains finally.

By comparing the prior-β grain size given in Table 1, the mean size of the equiaxed prior-β grains of each wall are in the order of wall A > wall C > wall B. It is more likely to promote the further growth of the prior-β grains to become coarse beyond the β-transus temperature. As a result, the prior-β grain size in wall A should be relatively larger than that of other two walls. In fact, wall C with the lowest tem-

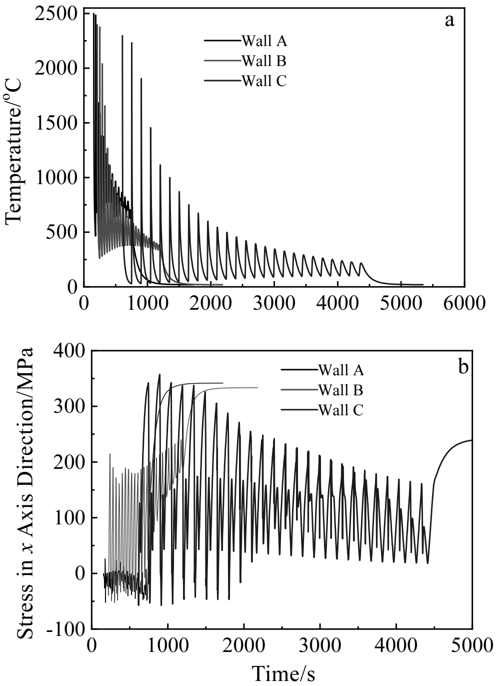

Fig.3 Calculated real-time thermal field (a) and longitudinal (travel direction) stress field (b) evolution of 5 mm from the top surface of the substrate

perature obtained the coarser prior-β grains than wall B. The mean prior-β grain size of wall C is also larger than that of wall B when the sixth layer is deposited for relatively lower nucleation rate and longer incubation time (Fig.2f and 2h), which indicates that higher stress and lower temperature also suppress the recrystallization of wall C. Wall B under the appropriate temperature and stress can ensure adequate storage energy and grain boundary migration, which can maximize the promotion of recrystallization. After recrystallization, the prior-β grains in the deposited walls are still very coarse, which indicates that under the temperature and stress conditions in the WAAM process, prior-β grain growth rate is more pronounced than the nucleation rate. This may be attributed to the following mechanisms. First, when heated above the β-transus temperature, the diffusion is considerably fast to promote the prior-β grain growth. Second, little alloy element or particle pin prior-β grain boundaries to hinder the grain growth of Ti-6Al-4V.

When six layers are deposited, the relative low-density dislocation and stored energy regions are mainly concentrated within recrystallization β grains. It is attributed to the nucleation and growth of recrystallized β grains that consume the dislocation and promote the dislocation movement from the interior of the prior-β grain to grain boundaries. As a result, relatively high-density dislocation occurs which is mainly concentrated in the prior-β grain boundaries (Fig.4b). It is interesting to note that not only recrystallization of the β grains occurred, but also the α phase recrystallized between the two adjacent α phase boundaries. The high dislocation density was sweep out and a dislocation free zone was formed within the newly created nuclei (Fig.4c).

The equiaxed prior-β grains convert to columnar prior-β grains along the deposition direction in wall A and wall B finally. With the increase of the deposition height, not only the storage energy provided by the stress is reduced, but also the heat accumulation and the low cooling rate consumes the most of the stored energy during the recovery process. After the favoring selection of prior-β grain growth, the columnar prior-β grains appear. In fact, it is more likely to form columnar prior-β grains by AMed titanium because the constitutional undercooling ahead of the solid/liquid interface is too insufficient to nucleate. The growth restriction factor Q is defined as the rate of development of undercooling and can be used to determine the size of grain refinement ability[17].

$$Q = m_l c_0 (k - 1) \tag{2}$$

where m_l is the slope of the liquidus, c_0 is the solute concentration in wt% and k is the partition coefficient. There is limited constitutional undercooling in Ti-6Al-4V for negligible growth restriction provided by aluminium and vanadium. The growth orientation of the coarse columnar prior-β grains is consistent with the maximum thermal gradient (G) within the melt pool[18]. The bidirectional travel direction leads to an alternating opposite direction of the thermal gradient, which makes the columnar prior-β grains grow vertically in wall A, while tilted away from the building direction by about 9° in wall B for the only forward travel direction. The relationship between primary dendritic spacing and cooling rate is expressed as follows[19]:

$$\lambda = A v^{-n} \tag{3}$$

where λ is the primary dendrite spacing (μm), v is the cooling rate (K/s), A and n are constants related to material, and n>0. Therefore, the width of columnar prior-β grains gradually increases for the lower cooling rate and causes some columnar prior-β grains to be eliminated inevitably. On the top surface (Fig.1b~1c), there is no equiaxed prior-β grains; therefore, no CET occurs. Based on the theories proposed by Lin et al[20], the calculated critical G between the equiaxed and columnar is about 1.01×10^5 K/m as shown in Fig.5.

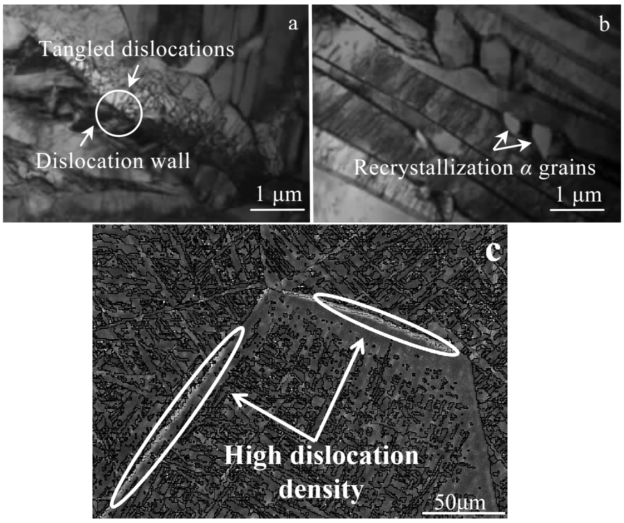

Fig.4 TEM images of corresponding to Fig.2f (a, b); the local misorientation distribution map of the equiaxed prior-β grains of Fig.2h (c)

Table 1 Size characteristics of equiaxed prior-β grains

Wall index	Mean grain size of equiaxed prior-β grains/μm	Prior-β grain aspect ratio
A	1186.6±415.61	1.14
B	1067.4±211.77	1.24
C	1096.9±169.2	1.51

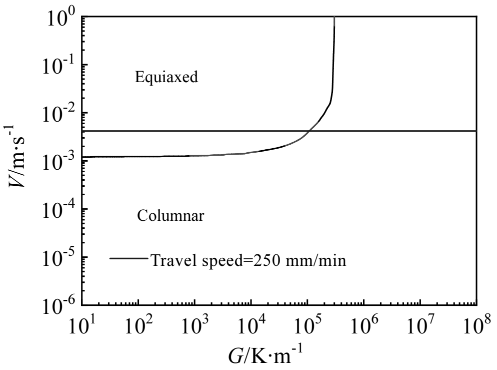

Fig.5 CET profile of Ti-6Al-4V alloy

3 Conclusions

1) Three Ti-6Al-4V walls are fabricated by WAAM with different deposition strategies. The bidirectional and unidirectional travel directions lead to different thermal gradient directions within the melt pool, and then the perpendicular and tilted growth of columnar prior-β grains are obtained, respectively.

2) The equiaxed prior-β grains are formed owing to the recrystallization, and the full equiaxed β grains can be obtained by extending the interlayer dwell time.

3) High temperature can promote the growth of prior-β grains. However, recrystallization is also another important factor that needs to be considered.

References

1 Lutjering G, Williams J C. *Titanium*[M]. Berlin: Springer, 2007: 8
2 Baufeld B, Biest O V D, Gault R. *International Journal of Materials Research*[J], 2009, 100: 1536
3 Donoghue J, Antonysamy A A, Martina F *et al. Materials Characterization*[J], 2016, 114: 103
4 Wu X, Liang J, Mei J *et al. Materials and Design*[J], 2004, 25: 137
5 Carroll B E, Palmer T A, Beese A M *et al. Acta Materialia*[J], 2015, 87: 30
6 Baufeld B, Biest O V D, Gault R. *Materials and Design*[J], 2010, 31: S106
7 Vilaro T, Colin C, Bartout J D. *Metallurgical and Materials Transactions A*[J], 2011, 42: 3190
8 Wang F, Williams S, Colegrove P *et al. Metallurgical and Materials Transactions A*[J], 2013, 44A: 968
9 Martina F. *Investigation of Methods to Manipulate Geometry, Microstructure and Mechanical Properties in Titanium Large Scale Wire+Arc Additive Manufacturing*[D]. Cranfield: Cranfield University, 2014
10 Colegrove P A, Donoghue J, Martina F *et al. Scripta Materialia*[J], 2017, 135: 111
11 Ren Y M, Lin X, Fu X *et al. Acta Materialia*[J], 2017, 132: 82
12 Humphreys F J, Hatherly M. *Recrystallization and Related Annealing Phenomena*[M]. Oxford: Elsevier, 2004
13 Qu F S, Zhou Y H, Zhang L Y *et al. Materials and Design*[J], 2015, 69: 153
14 Wang K, Liu G, Tao W *et al. Materials Characterization*[J], 2017, 126: 57
15 Szost B A, Terzi S, Martina F *et al. Materials and Design*[J], 2016, 89: 559
16 Wang J, Lin X, Wang J T *et al. Journal of Alloys and Compounds*[J], 2018, 768: 97
17 Bermingham M J, Kent D, Zhan H *et al. Acta Materialia*[J], 2015, 91: 289
18 Ladani L. *Metallurgical and Materials Transactions A*[J], 2015, 46: 3835
19 Zhong C, Chen J, Linnenbrink S *et al. Materials and Design*[J], 2016, 107: 386
20 Lin X, Li Y M, Wang M *et al. Science in China Series E: Technological Sciences*[J], 2003, 46: 475

电弧增材制造 Ti-6Al-4V 钛合金在不同扫描策略下的初生 *β* 晶组织宏观形态演变

王 健[1,2]，林 鑫[1,2]，薛爱堂[1,2]，周颖惠[1,2]，黄卫东[1,2]
(1. 西北工业大学 凝固技术国家重点实验室，陕西 西安 710072)
(2. 西北工业大学 金属高性能增材制造与创新设计工业和信息化重点实验室，陕西 西安 710072)

摘 要：基于电弧增材制造的方法，研究了不同沉积方向及层间间隔时间对电弧增材制造 Ti-6Al-4V 钛合金直壁墙的宏观组织特征的影响。双向扫描和单向扫描分别获得了竖直生长和倾斜生长的柱状初生 *β* 晶组织。通过增加层间间隔时间至 120 s 获得了全等轴初生 *β* 晶组织。结果表明，底部的等轴初生 *β* 晶组织的形成是由于发生了再结晶。等轴初生 *β* 晶组织的晶粒大小同时受到热循环和再结晶两方面因素的共同作用。

关键词：电弧增材制造；Ti-6Al-4V；初生*β*晶粒形态；再结晶

作者简介：王 健，男，1987 年生，博士生，西北工业大学材料科学与工程学院，陕西 西安 710072，E-mail: wanghealth@mail.nwpu.edu.cn